



ELSEVIER

The thermal rearrangement of $-\text{[Me}_2\text{Si-}\eta^5\text{-C}_5\text{H}_4(\text{CO})\text{Fe}(\text{CO})_2\text{Fe}(\text{CO})\text{-}\eta^5\text{-C}_5\text{H}_4\text{SiMe}_2\text{-}]$ in the presence of phosphorus ligands

Huailin Sun *, Xiangdang Teng, Xuebin Huang, Zhong Hu, Yanbin Pan

Department of Chemistry, Nankai University, Tianjin 300071, People's Republic of China

Received 15 June 1999; received in revised form 15 October 1999; accepted 15 October 1999

Abstract

Reaction of $-\text{[Me}_2\text{Si-}\eta^5\text{-C}_5\text{H}_4(\text{CO})\text{Fe}(\text{CO})_2\text{Fe}(\text{CO})\text{-}\eta^5\text{-C}_5\text{H}_4\text{SiMe}_2\text{-}]$ (**1**) with one equivalent of PR_3 in refluxing *p*-xylene for 9 h leads to rearranged products containing mainly $-\text{[Me}_2\text{Si-}\eta^5\text{-C}_5\text{H}_4\text{Fe}(\text{CO})_2\text{SiMe}_2\text{-}\eta^5\text{-C}_5\text{H}_4\text{Fe}(\text{CO})\text{PR}_3\text{-}]$ (**3**: R = OMe; **4**: R = OPh) and a small amount of $-\text{[Me}_2\text{Si-}\eta^5\text{-C}_5\text{H}_4\text{Fe}(\text{CO})_2\text{SiMe}_2\text{-}\eta^5\text{-C}_5\text{H}_4\text{Fe}(\text{CO})_2\text{-}]$ (**2**). When excess of PR_3 is used and/or the time of reaction is shortened, an intermediate product $-\text{[Me}_2\text{Si-}\eta^5\text{-C}_5\text{H}_4(\text{CO})\text{Fe}(\text{CO})_2\text{Fe}(\text{PR}_3)\text{-}\eta^5\text{-C}_5\text{H}_4\text{SiMe}_2\text{-}]$ (**5**: R = OMe; **6**: R = OPh) is obtained from the reaction. It is found that **5** and **6** rearrange much faster than **1** under the thermal condition leading to **3** and **4**, respectively. Crystal and molecular structures of **3** and **5** have been determined by X-ray diffraction methods. © 2000 Elsevier Science S.A. All rights reserved.

Keywords: Silicon; Iron; Rearrangement; Metathesis; Phosphorus; Substitution

1. Introduction

In 1993 [1], we reported a thermal rearrangement reaction of the cyclic structure $-\text{[Me}_2\text{Si-}\eta^5\text{-C}_5\text{H}_4(\text{CO})\text{Fe}(\text{CO})_2\text{Fe}(\text{CO})\text{-}\eta^5\text{-C}_5\text{H}_4\text{SiMe}_2\text{-}]$ (**1**). This reaction took place formally via metathesis between the Si–Si and Fe–Fe bonds of **1** to afford its rearranged isomer $-\text{[Me}_2\text{Si-}\eta^5\text{-C}_5\text{H}_4\text{Fe}(\text{CO})_2\text{SiMe}_2\text{-}\eta^5\text{-C}_5\text{H}_4\text{Fe}(\text{CO})_2\text{-}]$ (**2**) containing two Si–Fe bonds. However, it was found that this metathesis reaction did not take place for the intermolecular case between the Si–Si bond of $\text{Me}_3\text{SiSiMe}_3$, or $\text{PhMe}_2\text{SiSiMe}_2\text{Ph}$, and the Fe–Fe bond of $\eta^5\text{-C}_5\text{H}_5(\text{CO})\text{Fe}(\text{CO})_2\text{Fe}(\text{CO})\text{-}\eta^5\text{-C}_5\text{H}_5$ [1]. It was later found that this type of reaction did not occur for the intramolecular Si–Si and Fe–Fe bonds of the acyclic analog of **1**, e.g. $\text{Me}_3\text{SiMe}_2\text{Si-}\eta^5\text{-C}_5\text{H}_4(\text{CO})\text{Fe}(\text{CO})_2\text{Fe}(\text{CO})\text{-}\eta^5\text{-C}_5\text{H}_4\text{SiMe}_2\text{SiMe}_3$, under the thermal conditions [2]. Therefore, it was the cyclic

structure of **1** that appeared to be responsible for the metathetical rearrangement reaction.

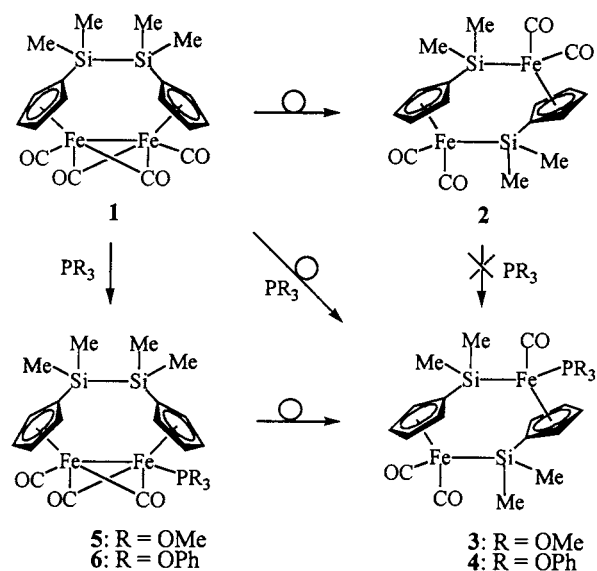
Subsequent studies have confirmed that this kind of reaction can occur for a wide variety of compounds with the similar cyclic structures [3–6]. Meanwhile, much progress has also been achieved in revealing the details of this reaction. A mechanism involving homolysis of the Fe–Fe bond to give two iron-centered radicals as the initial step (biradical mechanism) and subsequently either stepwise or concerted attack of the Si–Si bond by the iron radicals to form the two Si–Fe bonds has been proposed [4,6]. However, an obvious drawback exists for this mechanism because the alternative pathway involving formation of coordinatively unsaturated iron species via CO loss as the initial step of this reaction, which is equally possible to the biradical mechanism, has never been considered.

In order to gain further insight into the details of this reaction, we have carried out a study on the thermal rearrangement of **1** in the presence of phosphorus ligands. Our interests in this study stem from the fact that it may give us some information about whether the rearrangement reaction operates via the CO loss path-

* Corresponding author.

E-mail address: sunhl@nankai.edu.cn (H. Sun)

way. Results obtained in this study, however, seem unlikely to support the CO loss pathway. Although rearranged products containing phosphorus ligands are really obtained, these products are demonstrated to have come from rearrangements of the intermediate products formed via simple substitution of a carbonyl group for the phosphorus ligands prior to the rearrangement. Of particular interest is that these intermediate products have been isolated and found to undergo rearrangements much faster than **1**.



Scheme 1.

2. Results and discussion

2.1. Rearrangement reaction of **1** in the presence of phosphorus ligands

The rearrangement reaction of **1** in the presence of equivalent moles of trimethylphosphite is carried out in *p*-xylene at refluxing temperature, a condition under which the rearrangement of **1** has been well established to take place affording the rearranged product **2** [1]. In the presence of trimethylphosphite, however, a product that is different from **2** and later identified to be **3** is obtained in 50% yield from the reaction after 9 h of refluxing. Meanwhile, a small amount of **2** is also obtained, as well as a minimum amount of **1** recovered (Scheme 1). It is observed that an intermediate product with dark green color arises in the reaction process and disappears at the end of the reaction when TLC is used to monitor this reaction. When triphenylphosphite is used in place of trimethylphosphite in the above reaction, an intermediate product with a dark green color is also observed and disappears at the end of the reaction. After 9 h of refluxing, the product obtained is **4** in 72% yield. Meanwhile, a small amount of **2** is also obtained, as well as a little amount of **1** recovered (Scheme 1).

Compounds **3** and **4** are rearranged products of **1** in which one of the carbonyl groups is replaced by appropriate phosphorus ligands. IR spectra of **3** and **4** are taken and shown to give their respective three absorption bands in the region of the carbonyl stretching vibration. One of them appearing at a lower frequency (1901 cm^{-1} for **3**; 1911 cm^{-1} for **4**), is due to the stretching vibration of a carbonyl group bonded to the iron atom bearing the phosphorus ligands. The other two absorption bands at higher frequencies (1921 and 1984 cm^{-1} for **3**; 1921 and 1977 cm^{-1} for **4**), which are closely related to those of **2** (1925.8 and 1975.0 cm^{-1}), are attributed to symmetric and asymmetric stretching vibration of the two carbonyl groups at the other iron atom. The fact that the carbonyl group attached to the iron atom bearing a phosphorus ligand gives rise to the absorption band at a lower frequency than the other two carbonyl groups should be attributed to the electron-releasing effect of the phosphorus ligands [7]. This electronic effect can strongly enhance back donation of electrons from the iron atom to the vacant- π^* orbital of the carbonyl group, leading to strengthening of the iron-carbon bond and hence weakening of the carbon-oxygen multiple bond of the carbonyl group. $^1\text{H-NMR}$ spectra of **3** and **4** generally show four sharp singlets for Si-Me protons in the region of 0.22–0.59 ppm and some singlets due to eight different protons of the two C_5H_4 groups in the lower field region of 4.20–5.10 ppm. Other signals, due to protons of phosphorus ligands, are also in accord with the structures.

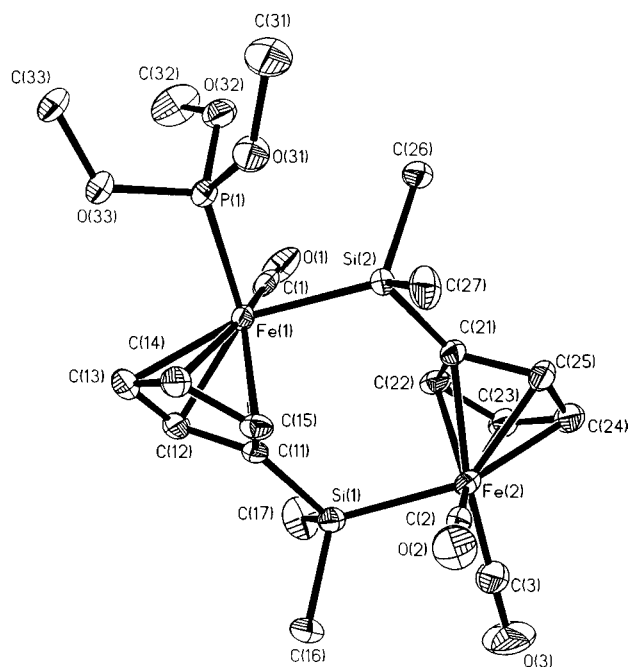


Fig. 1. Molecular structure of $[\text{Me}_2\text{Si-}\eta^5\text{-C}_5\text{H}_4\text{Fe}(\text{CO})_2\text{SiMe}_2\text{-}\eta^5\text{-C}_5\text{H}_4\text{Fe}(\text{CO})\text{PR}_3]\text{-}$ (**3**: R = OMe).

Table 1
Crystallographic data of **3** and **5**

	3	5
Formula	C ₂₀ H ₂₉ Fe ₂ O ₆ PSi ₂	C ₂₀ H ₂₉ Fe ₂ O ₆ PSi ₂
Formula weight	564.29	564.29
Crystal system	Monoclinic	Orthorhombic
Space group	P2 ₁	Pbca
Z	2	8
a (Å)	8.444(2)	10.804(2)
b (Å)	12.751(3)	13.710(3)
c (Å)	11.929(2)	32.850(7)
α (°)	90.00(0)	90.00(0)
β (°)	100.36(3)	90.00(0)
γ (°)	90.00(0)	90.00(0)
V (Å ³)	1263(1)	4866(2)
Radiation	Mo-K _α	Mo-K _α
λ (Å)	0.71073	0.71073
Temperature (K)	299 ± 1	299 ± 1
μ (mm ⁻¹)	1.3858	1.3342
R	0.039	0.055
R _w	0.043	0.058
Goodness-of-fit	0.85	0.97

The molecular structure of **3** has been determined by the X-ray diffraction method as shown in Fig. 1. The molecule in crystalline state has C₁ symmetry. The main body of the molecule is similar to its parent structure **2** reported previously [1], except that one of the carbonyl groups of **2** has been replaced by trimethylphosphite. The six-membered cyclic structure consisting of two silicon, two iron and two silicon-bonded cyclopentadi-

Table 2
Selected bond lengths (Å) and angles (°) of **3**

Bond lengths			
Fe(1)–Si(2)	2.305(2)	Fe(2)–Si(1)	2.313(2)
Fe(1)–C(1)	1.713(7)	Fe(2)–C(2)	1.752(10)
Fe(1)–P(1)	2.125(2)	Fe(2)–C(3)	1.742(8)
Fe(1)–C(11)	1.217(6)	Fe(2)–C(21)	2.113(7)
Fe(1)–C(12)	2.090(7)	Fe(2)–C(22)	2.087(7)
Fe(1)–C(13)	2.109(8)	Fe(2)–C(23)	2.073(9)
Fe(1)–C(14)	2.089(8)	Fe(2)–C(24)	2.092(10)
Fe(1)–C(15)	2.098(7)	Fe(2)–C(25)	2.100(8)
Si(1)–C(11)	1.883(6)	Si(2)–C(21)	1.896(7)
Si(1)–C(16)	1.874(9)	Si(2)–C(26)	1.881(8)
Si(1)–C(17)	1.877(11)	Si(2)–C(27)	1.884(9)
Bond angles			
Si(2)–Fe(1)–P(1)	86.7(2)	Si(1)–Fe(2)–C(2)	84.4(10)
Si(2)–Fe(1)–C(1)	83.9(8)	Si(1)–Fe(2)–C(3)	86.9(12)
P(1)–Fe(1)–C(1)	86.0(9)	C(2)–Fe(2)–C(3)	87.7(19)
Si(2)–Fe(1)–C(11)	101.3(5)	Si(1)–Fe(2)–C(21)	102.6(6)
Fe(2)–Si(1)–C(11)	111.9(9)	Fe(1)–Si(2)–C(21)	111.8(9)
Fe(2)–Si(1)–C(16)	115.4(10)	Fe(1)–Si(2)–C(26)	114.2(9)
C(11)–Si(1)–C(16)	101.4(11)	C(21)–Si(2)–C(26)	99.4(10)
Fe(2)–Si(1)–C(17)	114.9(8)	Fe(1)–Si(2)–C(27)	118.5(7)
C(11)–Si(1)–C(17)	105.3(12)	C(21)–Si(2)–C(27)	100.8(12)
C(16)–Si(1)–C(17)	106.5(14)	C(26)–Si(2)–C(27)	109.7(13)
Fe(1)–C(11)–Si(1)	132.3(14)	Fe(2)–C(21)–Si(2)	128.1(14)

enyl carbon atoms adopts a chair-like conformation, which is also similar to that of **2** [1]. It is found that the trimethylphosphite group occupies an equatorial position at the chair conformed ring. This is reasonable since the trimethylphosphite is much more bulky than the carbonyl ligand. The length of the Fe(1)–Si(2) (2.305(2) Å) bond bearing the phosphorus ligand is somewhat shorter than that of the other Fe(2)–Si(1) (2.313(2) Å) bond, while the latter has no obvious difference from the length of Fe–Si bonds (2.315(2) Å) of **2** [1] within the limit of experimental error. This difference between the lengths of the two Fe–Si bonds of **3** is attributed to the electronic effect of trimethylphosphite that has strengthened its neighboring Fe(1)–Si(2) bond. This situation is also found for the bond length between the iron and the CO-carbon atoms. Thus, the bond length of Fe(1)–C(1) (1.713(7) Å) is found to be slightly shorter than that of Fe(2)–C(2) (1.752(10) Å) and Fe(2)–C(3) (1.742(8) Å). These electronic effects of the phosphorus ligands consist with the results observed by IR spectra as stated above. All other bond lengths and angles are normal with respect to those reported for **2** [1]. Crystallographic data are presented in Table 1 and selected bond lengths and angles are presented in Table 2.

It is clearly shown that the rearrangement of **1** in the presence of phosphorus ligands leads to the rearranged products containing corresponding phosphorus ligands. This result is of much interest. It stimulates us to further examine the details of the reaction to see whether the formation of **3** and **4** comes from the rearrangement of **1** initiated by the CO loss and followed by the addition of the phosphorus ligands after the rearrangement having taken place.

2.2. Isolation of the intermediate products and their rearrangements

It is noted in the above reactions that there is always an unknown product with a green color that arises in the reaction process and disappears at the end of the reaction. In order to obtain the green compound, the reaction of **1** with trimethylphosphite is stopped after refluxing for only 4.5 h in another run. Simple separation of the products by column chromatography affords dark green crystals of **5** in 27% yield (Scheme 1). Our attempt to obtain the other intermediate product from the reaction of **1** with triphenylphosphite following the same procedure, however, was not successful due to its rather low yield. This difficulty is overcome when the procedures used above are changed. It is found that **5** can be obtained in much better (up to 74%) yield when excess trimethylphosphite is used in its reaction with **1** after refluxing in *p*-xylene for only 10 min. This result can be rationalized as this reaction is a bimolecular process and hence sensitive to the concen-

tration of the phosphorus ligand. According to such a principle, the reaction of **1** with an excess of triphenylphosphite was also carried out. In this situation, **6** is obtained in 15% yield after refluxing in *p*-xylene for 30 min (Scheme 1).

IR and ¹H-NMR spectra of **5** and **6** are recorded and found to be in accord with the structures. Thus, the IR

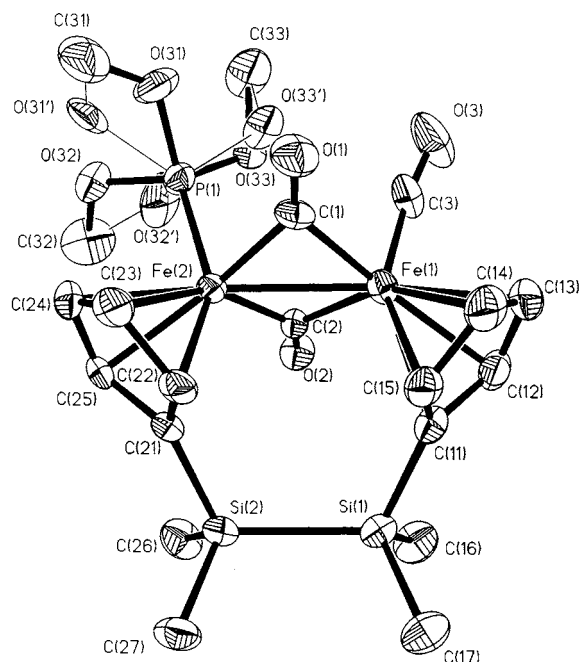


Fig. 2. Molecular structure of $[\text{Me}_2\text{Si}-\eta^5\text{-C}_5\text{H}_4(\text{CO})\text{Fe}(\text{CO})_2\text{-Fe}(\text{PR}_3)_2-\eta^5\text{-C}_5\text{H}_4\text{SiMe}_2]$ (**5**; R = OMe), in which disorder for the oxygen atoms of the trimethylphosphite ligand was observed.

Table 3
Selected bond lengths (Å) and angles (°) of **5**

Bond lengths			
Fe(1)–Fe(2)	2.522(1)	Si(1)–Si(2)	2.350(3)
Fe(1)–C(1)	1.935(7)	Fe(2)–C(1)	1.897(7)
Fe(1)–C(2)	1.957(7)	Fe(2)–C(2)	1.911(7)
Fe(1)–C(3)	1.731(8)	Fe(2)–P(1)	2.135(2)
Fe(1)–C(11)	2.152(7)	Fe(2)–C(21)	2.153(6)
Fe(1)–C(12)	2.118(7)	Fe(2)–C(22)	2.153(6)
Fe(1)–C(13)	2.095(8)	Fe(2)–C(23)	2.147(7)
Fe(1)–C(14)	2.150(9)	Fe(2)–C(24)	2.095(8)
Fe(1)–C(15)	2.154(7)	Fe(2)–C(25)	2.115(7)
Bond angles			
Fe(2)–Fe(1)–C(1)	48.2(2)	Fe(1)–Fe(2)–C(1)	49.5(2)
Fe(2)–Fe(1)–C(2)	48.5(2)	Fe(1)–Fe(2)–C(2)	50.1(2)
C(1)–Fe(1)–C(2)	94.1(3)	C(1)–Fe(2)–C(2)	96.8(3)
Fe(2)–Fe(1)–C(3)	104.9(3)	Fe(1)–Fe(2)–P(1)	104.0(1)
Fe(2)–Fe(1)–C(11)	107.8(2)	Fe(1)–Fe(2)–C(21)	107.6(2)
Fe(2)–P(1)–O(31)	119.5(1)	Fe(2)–P(1)–O(31')	121.4(1)
Fe(2)–P(1)–O(32)	119.0(1)	Fe(2)–P(1)–O(32')	117.8(1)
Fe(2)–P(1)–O(33)	117.8(1)	Fe(2)–P(1)–O(33')	115.9(1)
Si(2)–Si(1)–C(11)	113.3(2)	Si(1)–Si(2)–C(21)	113.6(2)
Fe(1)–C(1)–Fe(2)	82.3(3)	Fe(1)–C(2)–Fe(2)	81.4(3)
Fe(1)–C(11)–Si(1)	130.7(3)	Fe(2)–C(21)–Si(2)	129.4(3)

spectrum of **5** or **6** generally shows three absorption bands in the region of carbonyl stretching vibrations. One of them, which appears at a higher frequency (1948 cm^{-1} for **5** and 1961 cm^{-1} for **6**), corresponds to the stretching vibration of the terminal carbonyl group. The other two absorption bands (at 1770 and 1728 cm^{-1} for **5**, 1774 and 1735 cm^{-1} for **6**) are related to symmetric and asymmetric stretching vibration of two bridging carbonyl groups, respectively. ¹H-NMR spectra of **5** and **6** give their respective two sharp singlets for Si–Me protons at higher field (0.13–0.33 ppm) and four singlets for C₅H₄ groups at lower field (3.45–5.36 ppm). Other signals due to protons of phosphorus ligands are also in accord with the structures.

The molecular structure of **5** is determined by X-ray crystallographic study as shown in Fig. 2. It is found that **5** in crystalline state has C₁ symmetry. Lengths of both Fe(1)–Fe(2) (2.522(1) Å) and Si(1)–Si(2) (2.350(3) Å) bonds have no obvious difference from those of **1** (2.526(2) and 2.346(4) Å, respectively) previously reported [1]. The length of the Fe(1)–C(3) bond (1.731(8) Å) bearing a terminal carbonyl group is slightly shorter than corresponding bonds of **1** (1.75(1) and 1.77(1) Å). This is attributed to the presence of trimethylphosphite, which has a strong electron-releasing effect being transferred through the Fe–Fe bond to the other iron atom. This kind of effect is also observed for lengths of Fe(2)–C(1) (1.897(7) Å) and Fe(2)–C(2) (1.911(7) Å) bonds, which are slightly shorter than that of Fe(1)–C(1) (1.935(7) Å) and Fe(1)–C(2) (1.957(7) Å) bonds for the bridging carbonyl groups. It indicates that the effect of the phosphorus ligand is strengthening, rather than weakening its neighboring bonds. On the other hand, the steric effect of the bulky phosphorus ligand finds expression in the hindrance with its vicinal Cp group, which makes the dihedral angle between the two Cp planes of **5** (90.9°) 5.6° larger with respect to that of **1** (85.3°). The six-membered cyclic structure consisting of the two silicon, two iron and two silicon-bonded cyclopentadienyl carbon atoms adopts a slightly twisted boat conformation which is akin to that of **1**; other bond lengths and angles are normal with respect to those reported previously for **1** [1]. Crystallographic data are presented in Table 1 and selected bond lengths and angles are presented in Table 3.

It is obvious that **5** and **6** are derivatives of **1** in which one of the terminal carbonyl groups is replaced by phosphite ligands. Formation of these products in the above reaction is reasonable because this kind of substitution reaction has been well known to take place for analogs of **1** under thermal conditions [8,9]. On the other hand, the fact that **5** and **6** disappear at the end of the reaction (see above) is most probably due to the fact that they have been transformed to **3** and **4**, respectively. To get direct evidence for this transformation, **5** obtained above is put back into *p*-xylene and

subjected to further refluxing. After one and a half hours of refluxing, it is found that **5** is converted to **3** almost completely in 56% isolated yield (Scheme 1). This result shows that **5** can also rearrange under thermal conditions. Particularly, it is noted that the rearrangement of **5** is much faster than that of **1**. When **6** is allowed to rearrange under thermal conditions, it is found that this compound rearranges so fast that it can complete in only 15 min to give the final product **4** in 72% yield (Scheme 1). This should be part of the reason why the intermediate product **6** is difficult to obtain.

Thus formation of **3** and **4** in the above reactions can be explained reasonably as being first formation of the intermediate products **5** and **6**, and their subsequent rearrangements. However, an alternative pathway that involves first rearrangement of **1** to form **2** and subsequent substitution of a carbonyl group of **2** for the phosphorus ligands might also contribute to the formation of **3** and **4**. To test this possibility, **2** is refluxed with trimethylphosphite in *p*-xylene. After refluxing for 9 h, only a small amount of **3** (less than 1% yield) is obtained. Similar refluxing of **2** with triphenylphosphite in *p*-xylene for 9 h gives no noticeable amount of **4**. Although **3** is obtained from the reaction of **2** and trimethylphosphite, its rather low yield cannot compete with the very high yield of **3** obtained from the reaction of **1** with trimethylphosphite. This result shows that substituting of a carbonyl group of **2** for phosphorus ligands under thermal condition is much more difficult, and formation of **3** and **4** from **2** must be ruled out (Scheme 1).

2.3. Mechanistic consideration on the rearrangement process

Although it is demonstrated that **3** and **4** obtained in the reaction of **1** and the phosphorus ligands come from the rearrangements of the intermediate products **5** and **6**, whether the CO loss pathway contributes concurrently to the formation of **3** and **4** is still a question.

It has been found in a previous study [1] that the rearrangement of **1** gives only 60% yield of **2**. We note that this reaction is always accompanied by the formation of a large amount of intractable decomposition product even if it is performed very carefully under oxygen-free conditions. On the assumption that the CO loss pathway operated, the low yield of **2** should be due to CO escaping from the reaction system after its dissociation. Consequently, there would be insufficient CO to add to the vacant coordination site after rearrangement. Accordingly, it should be expected that the presence of additional phosphorus ligands in the reaction system might be helpful to improve the yield of the rearrangement products. However, it is found that the results obtained above do not agree with this hypothesis. As stated above, the presence of trimethylphosphite

in the rearrangement process of **1** does not lead to increased yield of **3**, whereas the higher yield of **4** obtained in the presence of triphenylphosphite ought to be attributed to the improved yield of the rearrangement of **6**. So, it is more probable that the rearrangement of **1** does not involve CO loss as the initial step, although it cannot be completely ruled out at the present stage.

It is of interest to note here that several rearrangements similar to that of **1** have been reported recently. In 1996, Bitterwolf et al. [10] reported a similar rearrangement of $-\text{[Me}_2\text{Si-}\eta^5\text{-C}_5\text{H}_4(\text{CO})_2\text{RuRu}(\text{CO})_2\text{-}\eta^5\text{-C}_5\text{H}_4\text{-}]$ (**7**) under photochemical condition to afford $-\text{[Me}_2\text{Si-}\eta^5\text{-C}_5\text{H}_4(\text{CO})_2\text{Ru-}\eta^5\text{-C}_5\text{H}_4\text{Ru}(\text{CO})_2\text{-}]$, in which the Ru–Ru and Cp–Si bonds have been broken and new Ru–Cp and Ru–Si bonds formed. Both CO loss and biradical pathways have been considered to explain this reaction. Furthermore, formation of the radicals from homolysis of the Ru–Ru bond has been trapped, although it is more difficult than usual cases. On the other hand, a detailed investigation on another similar rearrangement of $-\text{[}\eta^5\text{-C}_5\text{H}_4(\text{CO})_2\text{RuRu}(\text{CO})_2\text{-}\eta^5\text{-C}_5\text{H}_4\text{-}]$ (**8**) has been reported by Vollhardt's group [11] more recently. It is found that **8** can rearrange photochemically to afford $-\text{[}\eta^5\text{-C}_5\text{H}_4\text{Ru}(\text{CO})_2\text{-}\eta^5\text{-C}_5\text{H}_4\text{-Ru}(\text{CO})_2\text{-}]$, which involves cleavage of Ru–Ru and Cp–Cp bonds to give two Ru–C bonds. While there is no evidence for a radical mechanism observed in the rearrangement of **8**, it is found that a concerted mechanism involving a tetrahedral transition state is most probably followed. All of these novel rearrangements are very similar to each other in structural character. However, it should be noted that the rearrangement of **1** is substantially different from the reactions of **7** and **8** in that the former is a thermal process whereas the latter two are photochemical ones. In fact, it was found that **1** did not undergo the rearrangement reaction upon irradiation for 10 h using a high-pressure mercury lamp soon after its thermal rearrangement was discovered.

On the other hand, the rearrangement of **1** involves cleavage of the Si–Si bond by the transition metal atoms. The latter is currently one of the warmest topics in the field of organosilicon chemistry. This kind of cleavage of Si–Si bonds has been found to occur widely for complexes with polysilanyl groups bonded either directly to the transition metal atoms [12–16], or indirectly to the η^1 -methylene [17] and η^4 -butadiene ligands [18]. For all of these cases, cleavages of the stable Si–Si bonds have easily occurred via interaction with coordinatively unsaturated transition metal moieties formed via dissociation of appropriate ligands. Whether cleavage of the Si–Si bond in the present system also follows the same principle should be considered seriously. Noting that the Si–Si bond in the present system is linked to the η^5 -cyclopentadienyl ligands, which is somewhat

different from those in other systems, the present rearrangement should belong to an independent type among those reactions involving cleavage of Si–Si bonds.

In summary, the mechanism of the present reaction is far from easy to determine. There are many possible pathways that must be taken into consideration for this rearrangement reaction. They should at least include the CO loss pathway, as well as the stepwise or concerted biradical mechanism. A true metathesis process involving a double cleavage of the Si–Si and Fe–Fe bonds has never been ruled out. In addition, the concerted mechanism involving a tetrahedral transient state is attractive, particularly as it has most probably been followed by the rearrangement of **8**. All these possibilities must be tested precisely before any of them is ruled out, or finalized as the real one. For example, the CO loss pathway cannot be ultimately ruled out without further evidence, although it seems unlikely according to the present study. Evidence to show that the iron radicals from homolysis of the Fe–Fe bond are really able to cleave the Si–Si bond should also be offered before the biradical mechanism becomes acceptable. Related work is being carried out in our laboratory.

3. Experimental

3.1. General

All reactions were carried out under an argon atmosphere. Xylene was dried by refluxing with sodium in the presence of diphenylketone under argon and distilled before use. IR spectra were recorded on Nicolet 5DX FT-IR spectrometer, and ¹H-NMR spectra were taken on Bruker AC-P200 instrument. Compounds **1** and **2** were prepared as reported previously [1]. Other chemicals were purchased and used without further purification.

3.2. Reaction of **1** with P(OMe)₃

To a 100 ml flask equipped with a reflux condenser containing 0.234 g (0.5 mmol) of **1** and 0.062 g (0.5 mmol) of P(OMe)₃ was added 10 ml of *p*-xylene. The resulting solution was refluxed on an oil bath with magnetic stirring. After a period of 9 h, the reaction was stopped and allowed to cool to room temperature. The solvent was then removed by distillation under reduced pressure to give a solid residue. This residue was dissolved in a small amount of benzene and separated by preparative TLC (silica GF-254, ether–petroleum ether 1:6) to give three bands. The first band with a light yellow color afforded 6 mg (0.013 mmol, 2.6% yield) of **2** [1]; the second band also with a light yellow color gave 138 mg (0.25 mmol, 50% yield) of **3**;

the third band with a deep red color afforded 1 mg (0.003 mmol, 0.6% yield) of unreacted **1** [1]. For **3**: light yellow crystals, m.p. 111–113°C. Anal. Calc. for C₂₀H₂₉O₆Fe₂PSi₂: C, 42.57; H, 5.18. Found: C, 42.38; H, 5.47. ¹H-NMR (CDCl₃): δ 0.22 (s, 3H, SiMe), 0.40 (s, 3H, SiMe), 0.46 (s, 3H, SiMe), 0.53 (s, 3H, SiMe), 3.60 (d, *J* = 11.2 Hz, 9H, P(OMe)₃), 4.40 (s, 1H, Cp), 4.61 (s, 1H, Cp), 4.68 (s, 1H, Cp), 4.74 (s, 1H, Cp), 4.95 (s, 1H, Cp), 4.98 (s, 1H, Cp), 5.05 (s, 2H, Cp). IR (KBr, cm⁻¹): ν_{CO} 1984 (s), 1921 (s), 1901(s).

3.3. Reaction of **1** with P(OPh)₃

Following the same procedure used above, 0.234 g (0.5 mmol) of **1** and 0.155 g (0.5 mmol) of P(OPh)₃ were refluxed in 10 ml of *p*-xylene for 9 h. After removal of the solvent, the residue was dissolved in a small amount of benzene and separated by preparative TLC (silica GF-254, benzene–petroleum ether 1:2) to develop three bands. The first band with a light yellow color gives 2 mg (0.005 mmol, 1% yield) of **2** [1]; the second band also with a light yellow color affords 270 mg (0.36 mmol, 72% yield) of **4**; the third band with a deep red color affords 1 mg (0.003 mmol, 0.6% yield) of unreacted **1** [1]. For **4**: light yellow crystals, m.p. 159–160°C. Anal. Calc. for C₃₅H₃₅O₆Fe₂PSi₂: C, 56.01; H, 4.70. Found: C, 55.97; H, 4.41. ¹H-NMR (CDCl₃): δ 0.37 (s, 3H, SiMe), 0.49 (s, 3H, SiMe), 0.56 (s, 3H, SiMe), 0.59 (s, 3H, SiMe), 4.20 (s, 1H, Cp), 4.25 (s, 1H, Cp), 4.65 (s, 1H, Cp), 4.69 (s, 1H, Cp), 4.76 (s, 1H, Cp), 5.00 (s, 1H, Cp), 5.06 (s, 1H, Cp), 5.10 (s, 1H, Cp), 7.06 (m, 9H, Ph), 7.24 (m, 6H, Ph). IR (KBr, cm⁻¹): ν_{CO} 1977 (s), 1921 (s), 1911 (s).

3.4. Isolation of **5**

(a) Following the same procedure stated above, 0.468 g (1.0 mmol) of **1** and 0.124 g (1.0 mmol) of P(OMe)₃ were refluxed in 20 ml of *p*-xylene for 4.5 h. Removal of the solvent gave a solid residue, which was dissolved in a small amount of benzene and separated by column chromatography (neutral alumina, benzene). After a band containing a mixture of **3** and **1** was removed, a dark green band was collected, from which 150 mg (0.27 mmol, 27% yield) of **5** was obtained. For **5**: black crystals, m.p. 180–182°C. Anal. Calc. for C₂₀H₂₉O₆Fe₂PSi₂: C, 42.57; H, 5.18. Found: C, 42.21; H, 5.73. ¹H-NMR (CDCl₃): δ 0.31 (s, 6H, SiMe₂), 0.33 (s, 6H, SiMe₂), 3.53 (d, *J* = 11.2 Hz, 9H, P(OMe)₃), 4.19 (s, 2H, Cp), 4.38 (s, 2H, Cp), 5.11 (s, 2H, Cp), 5.27 (s, 2H, Cp). IR (KBr, cm⁻¹): ν_{CO} 1987 (w), 1948 (s), 1770 (m), 1728 (s).

(b) Following the same procedure used above, 0.234 g (0.5 mmol) of **1** and 0.248 g (2.0 mmol) of P(OMe)₃ were refluxed in 10 ml of *p*-xylene for 10 min. After removal of the solvent, the residue was dissolved in a

small amount of benzene and separated by column chromatography (neutral alumina, ether–petroleum ether 1:4). A dark green band was collected, from which 210 mg (0.37 mmol, 74% yield) of **5** was obtained.

3.5. Isolation of **6**

Following the same procedure stated above, 0.234 g (0.5 mmol) of **1** and 0.62 g (2.0 mmol) of P(OPh)₃ were refluxed in 10 ml of *p*-xylene for 0.5 h. After removal of the solvent, the residue was dissolved in a small amount of benzene and separated by column chromatography (neutral alumina, petroleum ether–dichloromethane 4:1). After a band containing a mixture of **4** and **1** was removed, a dark band was collected, from which 58 mg (0.13 mmol, 15% yield) of **6** was obtained. For **6**: black crystals, m.p. 170–172°C. Anal. Calc. for C₃₅H₃₅O₆-Fe₂PSi₂: C, 56.01; H, 4.70. Found: C, 56.26; H, 4.97. ¹H-NMR (CDCl₃): δ 0.13 (s, 6H, SiMe₂), 0.33 (s, 6H, SiMe₂), 3.45 (s, 2H, Cp), 4.42 (s, 2H, Cp), 4.66 (s, 2H, Cp), 5.36 (s, 2H, Cp), 7.13–7.28 (m, 15H, Ph). IR (KBr, cm⁻¹): ν_{CO} 1961 (s), 1774 (w), 1735 (s).

3.6. The rearrangement of **5**

Following the same procedure stated above, 100 mg (0.18 mmol) of **5** obtained above and 10 ml of *p*-xylene were refluxed on an oil bath with magnetic stirring for 1.5 h. Removal of the solvent gave a solid residue. This residue was dissolved in a small amount of benzene and separated by column chromatography (neutral alumina, ether–petroleum ether 1:6) to give a yellow band, from which 56 mg (0.10 mmol, 56% yield) of **3** was obtained.

3.7. The rearrangement of **6**

Following the same procedure used above, 50 mg (0.089 mmol) of **6** and 5 ml of *p*-xylene were refluxed on an oil bath with magnetic stirring for 15 min. After the solvent was removed, the solid residue was dissolved in a small amount of benzene and separated by column chromatography (neutral alumina, ether–petroleum ether 1:8) to give a yellow band, from which 36 mg (0.064 mmol, 72% yield) of **4** was obtained.

3.8. Reaction of **2** with P(OMe)₃

Following the same procedure used above, 0.117 g (0.25 mmol) of **2** and 0.124 g (1.0 mmol) of P(OMe)₃ were refluxed in 10 ml of *p*-xylene for 9 h. Similar treatment of the resulting solution and separation of the residue by preparative TLC (silica GF-254, ether–petroleum ether 1:6) give 1 mg (0.0018 mmol, 0.7% yield) of **3**, and most of the starting material **2** was recovered.

3.9. Crystallographic studies of **3** and **5**

Crystals of **3** and **5** suitable for X-ray analysis were obtained from a hexane–ether solution. All data were collected on an Enraf–Nonius CAD4 diffractometer equipped with graphite monochromated Mo–K_α radiation. The structures were solved by the direct phase determination method. Hydrogen atoms were not found. All non-hydrogen atoms were refined by full-matrix least-squares method with anisotropic thermal parameter. All calculations were performed on a PDP 11/4 computer using the SDP-PLUS program system. A summary of the crystallographic results has been given in Table 1 and selected bond lengths and angles for **3** and **5** shown, respectively, in Tables 2 and 3.

4. Supplementary material

Details of structural determination, including atomic coordinates and thermal parameters, a full list of bond lengths and angles, and additional data, have been deposited with the Cambridge Crystallographic Data Centre (no. 123383 for **3**; no. 123384 for **5**). Copies of this information may be obtained free of charge from the Director, CCDC, 12 Union Road, Cambridge, CB2 1EZ, UK [fax: +44-1223-336033; or e-mail: deposit@ccdc.cam.ac.uk or www: http://www.ccdc.cam.ac.uk].

Acknowledgements

The authors are indebted to the referees of this paper for their suggestion to prepare compound **6** using excess of the phosphorus ligand. Support of this work by the National Natural Science Foundation of China (projects 29604003 and 29872020) is also gratefully acknowledged.

References

- [1] H. Sun, S. Xu, X. Zhou, H. Wang, X. Yao, J. Organomet. Chem. 444 (1993) C41.
- [2] H. Sun, X. Zhou, X. Yao, H. Wang, Polyhedron 15 (1996) 4489.
- [3] X. Zhou, W. Xi, S. Xu, Chin. Chem. Lett. 7 (1996) 385.
- [4] X. Zhou, Y. Zhang, W. Xie, S. Xu, J. Sun, Organometallics 16 (1997) 3474.
- [5] B. Wang, S. Xu, X. Zhou, J. Organomet. Chem. 540 (1997) 101.
- [6] B. Wang, Y. Zhang, S. Xu, X. Zhou, Organometallics 16 (1997) 4620.
- [7] (a) C.A. Tolman, Chem. Rev. 77 (1977) 313. (b) M.M. Rahman, L.-Y. Liu, K. Eriks, A. Prock, W. P. Giering, Organometallics 8 (1989) 1.
- [8] (a) R.J. Haines, A.L. DuPreez, Inorg. Chem. 8 (1969) 1459. (b) R.J. Haines, A.L. DuPreez, J. Organomet. Chem. 21 (1970) 181. (c) F.A. Cotton, A.J. White, Inorg. Chem. 13 (1974) 1402.

- [9] M. Gray Cox, A.R. Manning, J. Organomet. Chem. 469 (1994) 189.
- [10] T.E. Bitterwolf, J.E. Shade, J.A. Hansen, A.L. Rheingold, J. Organomet. Chem. 514 (1996) 13.
- [11] (a) K.P.C. Vollhardt, T.W. Weidman, J. Am. Chem. Soc. 105 (1983) 1676. (b) R. Boese, J.K. Cammack, A.J. Adam, J. Matzger, K. Pflig, W.B. Tolman, K.P.C. Vollhardt, T.W. Weidman, J. Am. Chem. Soc. 119 (1997) 6757.
- [12] H.K. Sharma, K.H. Pannell, Chem. Rev. 95 (1995) 1351.
- [13] (a) Z. Zhang, R. Sanchez, K.H. Pannell, Organometallics 17 (1995) 2605. (b) K.H. Pannell, H.K. Sharma, R.N. Kapoor, F. Cervantes-Lee, J. Am. Chem. Soc. 119 (1997) 9315.
- [14] (a) G.P. Mitchill, T.D. Tilly, G.P.A. Yap, A.L. Rheingold, Organometallics 14 (1995) 5472. (b) G.P. Mitchill, T.D. Tilly, Organometallics 15 (1996) 3477.
- [15] K. Ueno, K. Nakano, H. Ogino, Chem. Lett. (1996) 459. (b) K. Ueno, A. Masuko, H. Ogino, Organometallics 16 (1997) 5023. (c) K. Ueno, M. Sakai, H. Ogino, Organometallics 17 (1998) 2138. (d) H. Tobita, H. Kurita, H. Ogino, Organometallics 17 (1998) 2844. (e) H. Tobita, H. Kurita, H. Ogino, Organometallics 17 (1998) 2850.
- [16] S. Nlate, E. Herdtweck, R.A. Fisher, Angew. Chem. Int. Ed. Engl. 35 (1996) 1861.
- [17] (a) K.H. Pannell, J.R. Rice, J. Organomet. Chem. 78 (1974) C35. (b) K.H. Pannell, S.P. Vincenti, R.C. Scott, Organometallics 6 (1987) 1593. (c) S. Sharma, R.N. Kapoor, F. Cervantes-Lee, K.H. Pannell, Polyhedron 10 (1991) 1177. (d) K.H. Pannell, T. Kobayashi, R.N. Kapoor, Organometallics 11 (1992) 2229. (e) S. Sharma, K.H. Pannell, Organometallics 12 (1993) 3979.
- [18] Y. Nakadaira, T. Kobayashi, H. Sakurai, J. Organomet. Chem. 165 (1979) 399.